Synthesis of wafer-scale hexagonal boron nitride monolayers free of aminoborane nanoparticles by chemical vapor deposition

2014 Nanotechnology 25 145604

(http://iopscience.iop.org/0957-4484/25/14/145604)

IOP Publishing Nanotechnology
Nanotechnology **25** (2014) 145604 (6pp) doi:10.1088/0957-4484/25/14/145604

Synthesis of wafer-scale hexagonal boron nitride monolayers free of aminoborane nanoparticles by chemical vapor deposition

Jaehyun Han, Jun-Young Lee, Heemin Kwon and Jong-Souk Yeo[1]

School of Integrated Technology, Yonsei University, Songdo-dong, Yeonsu-gu, Incheon 406-840, Korea
Yonsei Institute of Convergence Technology, Yonsei University, Songdo-dong, Yeonsu-gu, Incheon 406-840, Korea

E-mail: jongsoukyeo@yonsei.ac.kr

Received 3 November 2013, revised 28 January 2014
Accepted for publication 14 February 2014
Published 14 March 2014

Abstract

Hexagonal boron nitride (h-BN) has gained great attention as a two-dimensional material, along with graphene. In this work, high-quality h-BN monolayers were grown in wafer scale (7×7 cm^2) on Cu substrates by using low-pressure chemical vapor deposition (LPCVD). We created h-BN monolayers that were free of polymeric aminoborane (BH_2NH_2) nanoparticles, which are undesirable by-products of the ammonia borane precursor, by employing a simple filtering system in the CVD process. The optical band gap of 6.06 eV and sharp and symmetric Raman peak measured at 1371 cm^{-1} indicate the synthesis of monolayer h-BN. In addition, spherical aberration (C_S)-corrected high-resolution transmission electron microscopic images confirm the production of a single-layer hexagonal array of boron and nitrogen atoms.

Keywords: hexagonal boron nitride, 2D material, chemical vapor deposition, filter, monolayer

(Some figures may appear in colour only in the online journal)

1. Introduction

Recently, hexagonal boron nitride (h-BN), a III–V compound of boron and nitrogen with strong covalent sp^2 bonds, has gained great interest as a two-dimensional (2D) material, following the discovery of graphene [1–3]. h-BN is a two-dimensional insulating material with a large direct band gap, up to 6 eV, while graphene has semi-metallic properties due to the electronic structure, with zero band gap energy [4–6]. Its layers have a weak van der Waals interaction between them, and properties such as its strong mechanical strength, high thermal conductivity, and chemical stability have been reported to be similar or superior to those of graphene [7–11]. Because of these excellent properties, h-BN can potentially be used for variety of applications such as dielectric layers, deep UV optoelectronic devices, and protective transparent substrates [4, 12, 13]. The ultra flat and charge impurity-free surface of h-BN is also an ideal substrate for two-dimensional materials such as graphene to maintain their electrical properties [14].

Several approaches have been used to synthesize single-layered or few-layered h-BN, such as exfoliating h-BN flakes [15] and unzipping boron nitride nanotubes [16], but the chemical vapor deposition method (CVD) has been widely used more recently since it is difficult to achieve controllable and massive fabrication of monolayer h-BN with other synthesis methods [10, 17, 18]. In the CVD method, the h-BN layer is grown on a metallic substrate such as Cu or Ni at a high temperature of about 1000 °C and transferred to a substrate of interest. Ammonia borane (BH_3NH_3) or borazine ($(HBNH)_3$) is used as the precursor, having a 1:1 ratio of boron and nitrogen. Borazine makes very thick h-BN with 5–50 layers and it is unstable at ambient conditions, which makes unsuitable for controllable growth of h-BN layers [17]. Therefore, ammonia borane has been widely used as a precursor in order to carry out controlled synthesis of single-layer h-BN [19–22]. Ammonia borane decomposes into hydrogen (gas), monomeric aminoborane (solid), and borazine (gas) that

[1] Author to whom any correspondence should be addressed.

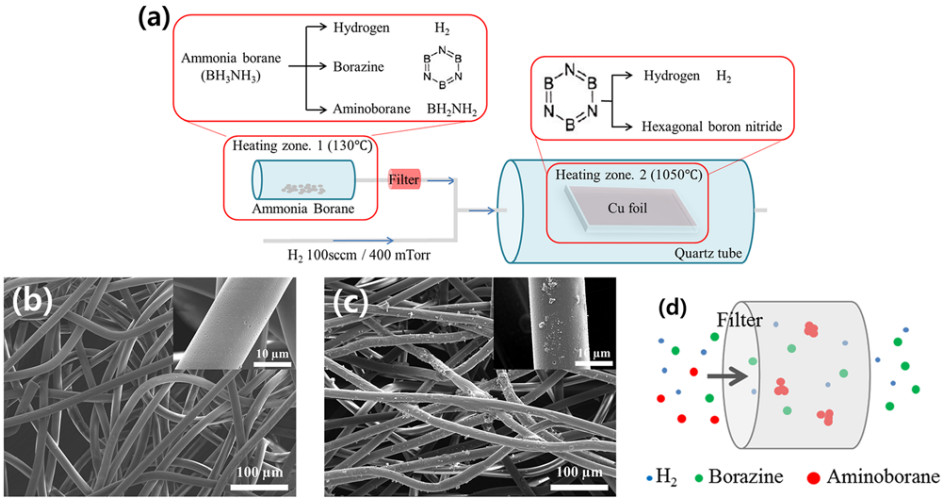

Figure 1. (a) Schematic diagram describing the CVD system and the two-step decomposition process of ammonia borane in the two heating zones. SEM images of an initial filter (b) and a used filter (c). Scale bar of larger images = 100 μm, inner one = 10 μm. (d) Schematic diagram of the filtering system.

is used for growing the h-BN layers [23–25]. However, very active monomeric aminoborane forms polymeric aminoborane nanoparticles that are white non-crystalline BN nanoparticles of 50–100 nm in diameter and stable at ambient conditions [19]. The presence of these BN nanoparticles following the synthesis has been hampering the implementation of h-BN in various applications [26]. Therefore, it is quite important to grow a clean and high-quality h-BN layer free of BN particles without having to introduce complicated process steps.

Here, we report the synthesis of wafer-scale high-quality single-layer h-BN without BN nanoparticles using a low-pressure CVD (LPCVD) method by employing filter paper to prevent the introduction of monomeric aminoborane onto the Cu substrate where the h-BN grows. Ammonia borane and Cu are used as the precursor and the substrate, respectively.

2. Experimental details

Figure 1(a) is a schematic diagram of our CVD system, with an illustration of the two-step decomposition process of ammonia borane for the synthesis of single-layer h-BN. The Cu substrate (99.98% pure and 25 μm thick) is placed in the middle of heating zone 2 (quartz tube with a 100 mm in diameter) first, and then the furnace temperature is set to 1050 °C with H_2 flow at 100 sccm (400 mTorr) for 1 h to remove CuO and to anneal the Cu substrate. Ammonia borane in a source bottle is placed in heating zone 1, and then heated to 130 °C by using a heating belt in order to provide suitable conditions for decomposing the precursor into hydrogen, monomeric aminoborane, and borazine [25]. The borazine diffuses from heating zone 1 to heating zone 2 and is then adsorbed on the Cu foil. The gas diffusion line is covered completely by the heating belt to maintain its temperature at 130 °C. Through the thermal decomposition and processes depicted in figure 1(a), an h-BN layer starts to grow across the whole surface of the Cu substrate, and the process is continued for 1 h. The initially nucleated and crystallized h-BN layer acts as an inert blanket, limiting further growth of an h-BN layer on top of the initial one. As a result, the h-BN mainly grows further in the horizontal, not vertical, direction, due to the self-terminating growth mode, as is usually seen in graphene [20, 27]. The surface morphology and thickness of the h-BN layer were evaluated by field emission scanning electron microscopy (FE-SEM: JEOL, JSM-7100F) and atomic force microscopy (AFM: Park Systems, XE-100), respectively. The single layer h-BN on the Cu substrate was transferred to proper substrates (quartz and SiO_2/Si) in order to analyze the relevant characteristics. The vibration modes and binding energy of the boron and nitrogen atoms were analyzed by Raman spectroscopy (Horiba, Lab Ram ARAMIS) and x-ray photoelectron spectroscopy (XPS: Thermo Scientific, K-Alpha), respectively. The absorption spectrum and optical band gap of h-BN were measured with a UV–visible spectrophotometer (Agilent, Cary 5000). Spherical aberration (C_S)-corrected high-resolution transmission electron microscopy (C_S-corrected HRTEM: JEOL, JEM-ARM 200F) was used to verify the quality of the h-BN layer with atomic resolution images.

3. Results and discussion

In the growth process, BN particles formed by monomeric aminoborane are also transported along with borazine and H_2 gas as a driving force from heating zone 1 to heating zone 2. As a result, monolayer h-BN and BN nanoparticles are synthesized on the Cu substrate at the same time. Using a lower decomposition temperature (under 130 °C) can lead to a milder pyrolysis of the source to reduce the gas flow, which tends to provide a smaller amount of BN nanoparticles. Thus heavier BN nanoparticles can be restricted from diffusing far enough to reach the Cu surface [19]. However, this method is not efficient in synthesizing large-scale and controllable monolayer h-BN, as the amount of borazine source decreases rapidly with lower decomposition temperature (under 130 °C) [25].

In this study, we adopted a rather simple filtering system to effectively remove the BN nanoparticles while allowing the maximum amount of borazine with sufficiently high

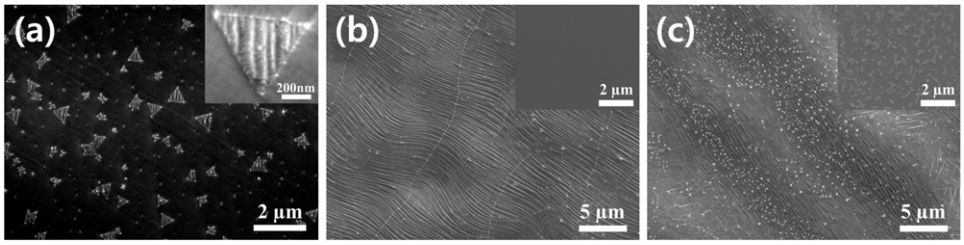

Figure 2. (a) SEM images of triangular h-BN on a Cu substrate, grown for 15 min. (b) and (c) SEM images of fully covered h-BN on Cu (larger images) and transferred onto SiO_2/Si (images inside) without BN nanoparticles (b) and with many BN particles (c), grown for 1 h, respectively.

decomposition temperature. To make high-quality h-BN without BN nanoparticles, monomeric aminoborane should be restricted before reaching to Cu substrate, which can be achieved by a filtering system. Figures 1(b) and (c) are SEM images of the filters, initially and after use, respectively, where the images inside are taken from a single strand within each filter. The filters provide an entangled open mesh structure composed of many strands having a clean surface with average diameter 15 μm, as shown in figure 1(b). In contrast, as observed from the image in figure 1(c), many BN nanoparticles are formed on the filter strands after use. Since monomeric aminoboranes are very active and unstable, they nucleate and grow as BN nanoparticles preferentially on the filter strands with higher surface energy. With the filter providing sufficiently thick meshes of the strands, most of the aminoborane nanoparticles are trapped while the H_2 and borazine can easily pass through. The filtering process of the BN nanoparticles is schematically shown in figure 1(d).

Figure 2(a) shows a triangular shape of h-BN islands nucleated initially for 15 min, before all the area of Cu substrate gets deposited with h-BN. A triangular shape is formed, because the nitrogen-terminated edges of the triangle are energetically more stable than boron-terminated edges, in contrast to the hexagonal shape generally observed in the case of graphene [28]. In addition, we also observe some nucleation sites from which h-BN continues to grow, and some islands formed by the coalescence of the triangular nanostructures. To cover the whole Cu substrate from such nucleation, growth, and coalescence, the h-BN layer was usually grown for 1 h. Figures 2(b) and (c) show SEM images of h-BN grown on a Cu substrate with and without utilizing the filter system, respectively. The smaller images inside the figures are from h-BN layers transferred onto 300 nm thick SiO_2 on Si, each with and without the filter. The commonly used etch-based transfer method with PMMA coating was used to achieve the transfer of h-BN to an arbitrary substrate [10]. Using the process described herein, h-BN was grown on Cu, uniformly covering the substrate. The wrinkles of the h-BN layer that are clearly observed are due to the negative thermal expansion coefficients of h-BN, as is also seen with graphene [19]. When h-BN grown at high temperature on a Cu substrate is cooled to a room temperature, the h-BN expands and the Cu shrinks, resulting in such wrinkles. SEM images of figure 2(b) show a relatively clean h-BN layer on the Cu substrate and also a very clean h-BN layer without BN nanoparticles transferred onto SiO_2/Si. Even though a limited amount of BN nanoparticles may pass through the filter, they cannot effectively reach the Cu substrate to form BN nanoparticles as the flux of H_2 and borazine gases transporting BN nanoparticles is also restricted by the filter [21, 22]. In contrast, the h-BN layer (figure 2(c)) synthesized without a filter shows too many BN nanoparticles on the Cu substrate and also on the SiO_2/Si substrate even after the transfer. These results demonstrate that BN nanoparticles can be simply and effectively removed by placing a filter after a gas line from heating zone 1 and before reaching heating zone 2, where the Cu substrate is located.

By incorporating a filter, a clean h-BN layer free of BN nanoparticles was grown on a Cu substrate with size as large as 7×7 cm^2, and then the whole h-BN layer was transferred onto a 6 in SiO_2/Si wafer. Figure 3(a) is a photograph of the layer transferred onto the wafer. The h-BN layer is marked by a dotted line since it is difficult to notice the h-BN layer due to the high optical transparency, with its wide band gap energy, up to 6 eV [29]. Raman spectroscopy is a powerful technique to analyze the characteristics of h-BN layers using the vibrational modes of boron and nitrogen (E_{2g} phonon mode) [30]. It is well known that a bulk Raman peak appears at 1366 cm^{-1} and shifts to a higher frequency as the number of h-BN layers decreases. The Raman peak for the E_{2g} phonon mode from single-layer h-BN is known to be at 1371 cm^{-1} [29]. Its highly symmetric Raman peak usually indicates a high-purity h-BN single layer, since by-products of borazine such as c-BN, $B_xC_yN_z$, and BN nanoparticles lead to an asymmetric Raman peak at 1370 cm^{-1} [22, 31]. Figure 3(b) shows the measured Raman spectra from nine different positions on the h-BN layer to check the uniformity in the quality of h-BN layer, using the Raman shifts measured with a 532 nm laser. Every Raman peak is located at about 1371–1372 cm^{-1}, and its shape is very sharp and symmetric, which indicates that the h-BN is grown as a high-purity monolayer. The symmetric Raman peak at 1372 cm^{-1} also proves that no carbon-based impurities are introduced into the chamber with the filtering paper. If there were any carbon contamination, the Raman spectrum should either show a broader graphene D band at 1360 cm^{-1} from a hybridized atomic monolayer (h-BNC) of graphene and h-BN or a broad peak between 1320 and 1350 cm^{-1} from boron carbon nitride ($B_xC_yN_z$), respectively [31, 32]. AFM was used to characterize the surface morphology and the thickness of h-BN layer further. Figure 3(c) provides AFM height profile images from the four edges of the square h-BN layer transferred onto the SiO_2/Si wafer shown in figure 3(a).

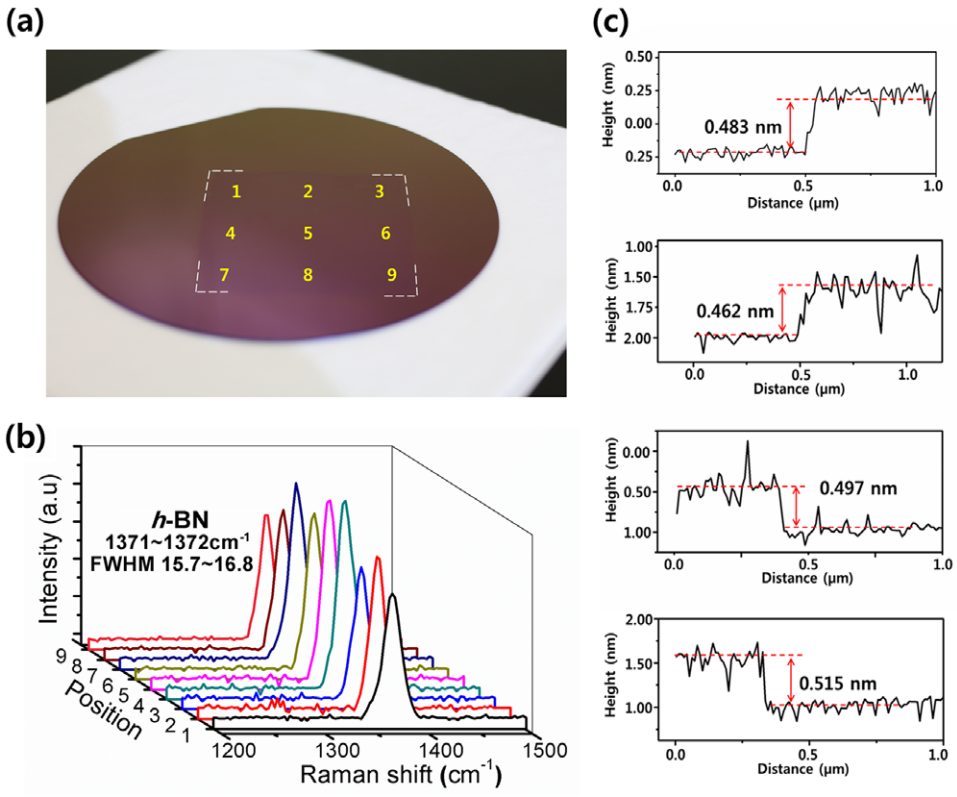

Figure 3. (a) Photograph of large-size h-BN (7×7 cm^2) transferred onto a 6 in SiO_2/Si wafer. (b) Monolayer h-BN Raman spectra from nine positions of the sample shown in (a). (c) The AFM height profiles on the four edges of the h-BN monolayer on SiO_2/Si shown in (a).

The overall thickness of the h-BN layer was measured to be from 0.462 to 0.515 nm, which agrees well with the reported thickness for single-layer h-BN [20].

X-ray photoelectron spectroscopy (XPS) was employed to verify the stoichiometry of boron and nitrogen in the single-layer h-BN. As shown in figures 4(a) and (b), the binding energies of B 1s and N 1s were measured as 190.18 eV and 398.28 eV, respectively, which are equal to those of bulk h-BN [21]. The atomic ratio of boron and nitrogen was measured to be 1:1.01, verifying the stoichiometry of h-BN. In order to analyze the optical properties and optical band gap (OBG) of the h-BN layer, the UV–visible absorption spectra were measured, resulting in almost zero absorbance in the visible light range, and without any strong excitonic peak around 215 nm, the wavelength corresponding to 5.7 eV reported to originate from symmetry-breaking effects such as dislocations or defect-related photoluminescence of h-BN (figure 4(c)) [12]. This result may indicate that the h-BN is synthesized in a highly symmetric and defect-free hexagonal structure [33, 34]. While the two-dimensional system of an h-BN layer requires an analysis that is different from that for a bulk material, the formula for a direct band gap semiconductor has been used to estimate the OBG of the h-BN film [22, 35]. The resultant band gap energy of 6.06 eV shown in figure 4(d) closely matches the theoretical value for monolayer h-BN [36], thus providing additional confirmation for its layer quality and thickness.

C_S-corrected HRTEM was used to observe the atomic structure of the single-layer h-BN directly after it was transferred onto the Cu mesh grid. Figure 5(a) is an atomic resolution image of h-BN, showing the unique hexagonal lattice structure of the material. The lattice constant estimated from the image is around 0.25 nm, which is very similar to a previously published value [15]. Using HRTEM operating at 80 kV, we clearly observed the honeycomb lattice structure of atomic boron and nitrogen sites from the single-layer h-BN. Figure 5(b) shows a triangular defect of h-BN formed by damage from the electron beam during the TEM analysis. This defect results from the difference in knock-on threshold energy for boron (74 keV) and nitrogen (84 keV) [15]. Boron atoms are damaged first by an accelerated electron beam due to their lower knock-on threshold energy than that of nitrogen atoms, which generates a vacancy of a boron atom. Due to the absence of bonding with a boron atom, neighboring nitrogen atoms can become unstable and easily removed, which in turn affects the next neighboring atoms sequentially. Therefore, a single boron vacancy can end up expanding to a larger triangular defect. In the synthesis of h-BN without the filter system, non-crystalline BN nanoparticles were observed to have diameters in the range 20–100 nm, as in figure 5(c). Characterization of the h-BN layer by C_S-Corrected HRTEM provides additional confirmation that high-quality single-layer h-BN has been synthesized by our CVD process.

4. Conclusions

In summary, we have demonstrated the synthesis of a high-quality h-BN monolayer in wafer-scale size of 7×7 cm^2 by

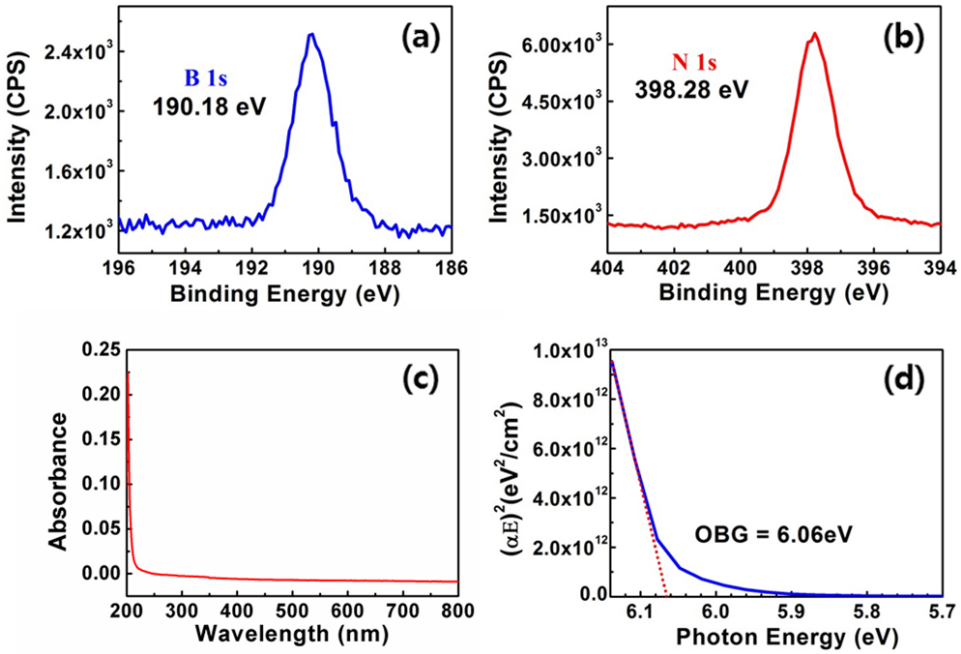

Figure 4. XPS spectra on (a) boron and (b) nitrogen of h-BN transferred onto the SiO_2/Si substrate. UV–visible absorption spectra of monolayer h-BN on a quartz substrate (c). (d) Optical band gap analysis of monolayer h-BN calculated from (c).

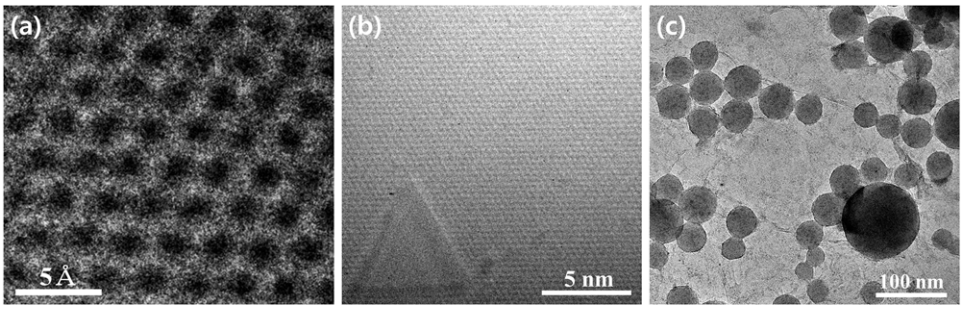

Figure 5. (a) Atomic resolution TEM images of single-layer h-BN. (b) Triangular defect from HRTEM images of h-BN. (c) TEM image of non-crystalline BN nanoparticles synthesized without using a filter.

using a CVD method incorporating a simple filter system. Investigations showed that the filter can effectively remove BN nanoparticles by restricting them from reaching the Cu substrate. A layer thickness of about 0.48 nm, measured by AFM, a Raman shift of 1371–1372 cm^{-1}, measured by micro Raman spectroscopy, along with an optical band gap of 6.06 eV estimated from UV–visible spectrophotometry confirmed the formation of monolayer h-BN. Quantitative XPS analysis of the ratio of boron and nitrogen and C_S-corrected HRTEM atomic resolution images of the hexagonal lattices indicated high-quality stoichiometric h-BN. The method presented here provides a promising technique for the synthesis of high-quality monolayer h-BN free of BN nanoparticles.

Acknowledgments

This research was supported by the MSIP (Ministry of Science, ICT and Future Planning), Korea, under the 'IT Consilience Creative Program' (NIPA-2014-H0201-14-1001) supervised by the NIPA (National IT Industry Promotion Agency). This research was also partially supported by a grant from the Joint Program for Samsung Electronics–Yonsei University.

References

[1] Paine R T and Narula C K 1990 *Chem. Rev.* **90** 73–91
[2] Corso M, Auwarter W, Muntwiler M, Tamai A, Greber T and Osterwalder J 2004 *Science* **303** 217–20
[3] Lee C, Li Q, Kalb W, Liu X Z, Berger H, Carpick R W and Hone J 2010 *Science* **328** 76–80
[4] Kubota Y, Watanabe K, Tsuda O and Taniguchi T 2007 *Science* **317** 932–4
[5] Lauret J S, Arenal R, Ducastelle F, Loiseau A, Cau M, Attal-Tretout B, Rosencher E and Goux-Capes L 2005 *Phys. Rev. Lett.* **94** 037405
[6] Geim A K and Novoselov K S 2007 *Nature Mater.* **6** 183–91
[7] Zhi C, Bando Y, Tang C, Kuwahara H and Golberg D 2009 *Adv. Mater.* **21** 2889–93
[8] Sevik C, Kinaci A, Haskins J B and Cagin T 2012 *Phys. Rev.* B **86** 075403

[9] Shi Y *et al* 2010 *Nano Lett.* **10** 4134–9
[10] Song L *et al* 2010 *Nano Lett.* **10** 3209–15
[11] Zhi C Y, Bando Y, Terao T, Tang C C, Kuwahara H and Golberg D 2009 *Chem. Asian J.* **4** 1536–40
[12] Watanabe K, Taniguchi T and Kanda H 2004 *Nature Mater.* **3** 404–9
[13] Watanabe K, Taniguchi T, Niiyama T, Miya K and Taniguchi M 2009 *Nature Photon.* **3** 591–4
[14] Dean C R *et al* 2010 *Nature Nanotechnol.* **5** 722–6
[15] Meyer J C, Chuvilin A, Algara-siller G, Biskupek J and Kaiser U 2009 *Nano Lett.* **9** 2683–9
[16] Zeng H, Zhi C, Zhang Z, Wei X, Wang X, Guo W, Bando Y and Golberg D 2010 *Nano Lett.* **10** 5049–55
[17] Kim K K, Hsu A, Jia X, Kim S M, Shi Y, Dresselhaus M, Palacios T and Kong J 2012 *ACS Nano* **6** 8583–90
[18] Ismach A *et al* 2012 *ACS Nano* **6** 6378–85
[19] Kim K K *et al* 2012 *Nano Lett.* **12** 161–6
[20] Kim G, Jang A R, Jeong H Y, Lee Z, Kang D J and Shin H S 2013 *Nano Lett.* **13** 1834–9
[21] Guo N, Wei J, Fan L, Jia Y, Liang D, Zhu H, Wang K and Wu D 2012 *Nanotechnology* **23** 415605
[22] Gao Y, Ren W, Ma T, Liu Z, Zhang Y, Liu W B, Ma L P, Ma X and Cheng H M 2013 *ACS Nano* **7** 5199–206
[23] Wolf G, Baumann J, Baitalow F and Hoffmann F P 2000 *Thermochim. Acta* **343** 19–25
[24] Baitalow F, Baumann J, Wolf G, Jaenicke-Rossler K and Leitner G 2002 *Thermochim. Acta* **391** 159–68
[25] Frueh S, Kellett R, Mallery C, Molter T, Willis W S, King'ondu C and Suib S L 2011 *Inorg. Chem.* **50** 783–92
[26] Wang Y, Yamamoto Y, Kiyono H and Shimada S 2009 *J. Am. Ceram. Soc.* **92** 787–92
[27] Paffett M T, Simonson R J, Papin P and Paine R T 1990 *Surf. Sci.* **232** 286–96
[28] Liu Y, Bhowmick S and Yakobson B I 2011 *Nano Lett.* **11** 3113–6
[29] Gorbachev R V *et al* 2011 *Small* **7** 465–8
[30] Zhi C, Bando Y, Tang C, Golberg D, Xie R and Sekigushi T 2005 *Appl. Phys. Lett.* **86** 213110
[31] Lee K H, Shin H J, Lee J, Lee I Y, Kim G H, Choi J Y and Kim S W 2012 *Nano Lett.* **12** 714–8
[32] Ci L *et al* 2010 *Nature Mater.* **9** 430–5
[33] Wirtz L, Marini A, Gruning M, Attaccalite C, Kresse G and Rubio A 2008 *Phys. Rev. Lett.* **100** 189701
[34] Museur L, Feldbach E and Kanaev A 2008 *Phys. Rev.* B **78** 155204
[35] Yuzuriha T H and Hess D W 1986 *Thin Solid Films* **140** 199–207
[36] Blase X, Rubio A, Louie S G and Cohen M L 1995 *Phys. Rev.* B **51** 6868–75